Exploring Orbital Mechanics Through Computational Problem-Solving

SN : 23099743

December 19, 2025

Abstract

This project investigates the gravitational interactions in multi-body systems using numerical integration techniques. We will examine the motion of systems with varying mass ratios, including two-body and three-body systems. By using Euler's method, the velocity Verlet method, and the Runge-Kutta integrator, we simulate the orbits, analyse energy conservation, and assess the accuracy and stability of these methods when varying quantities such as mass and time step. The study highlights the impact of different time steps on the conservation laws and compares the performance of these numerical techniques in modelling gravitational dynamic problems.

1 Introduction

Gravitational systems, such as moons orbiting planets or stars orbiting around their centre of mass, follow complex dynamics that we model using numerical methods.Understanding these systems is crucial for celestial mechanics, particularly when analytical solutions are difficult to obtain. This project investigates the motion of two and three-body systems by applying various numerical integration techniques, including the Euler method, velocity Verlet, and the higher-order Runge-Kutta method. Our primary focus is on simulating orbits, checking for conservation of energy and angular momentum, and evaluating the stability and accuracy of the methods used. By comparing different approaches, this study aims to deepen our understanding of numerical simulations in gravitational systems.

2 Preliminary Knowledge: Gravitational Force and Potential Energy

Before implementing any numerical integration methods, we define the forces that act on the bodies.

The gravitational force on a body m_1 at position $\mathbf{r}_1$ due to another mass m_2 at position $\mathbf{r}_2$ is given by Newton's law of gravitation:

$$\mathbf{F}_{12} = \frac{Gm_1m_2}{|\mathbf{r}_{12}|^3}\mathbf{r}_{12} \quad [1] \tag{1}$$

where $\mathbf{r}_{12} = \mathbf{r}_2 - \mathbf{r}_1$ is the displacement vector between the two masses, and G is the gravitational constant.

The potential energy U of the system is the sum of the gravitational potential energies between each pair of bodies:

$$U = \sum_i \sum_{j>i} \left(-\frac{Gm_im_j}{|\mathbf{r}_{ij}|} \right) \quad [2] \tag{2}$$

The total kinetic energy T of the system is the sum of the kinetic energies of each body:

$$T = \sum_i \frac{1}{2} m_i v_i^2 \quad [3] \tag{3}$$

where v_i is the velocity of body i.

The total force acting on a body m_i from all other bodies in the system is the vector sum of all pairwise gravitational forces:

$$\mathbf{F}_i = \sum_{j \neq i} \frac{G m_i m_j}{|\mathbf{r}_{ij}|^3} \mathbf{r}_{ij} \tag{4}$$

where $\mathbf{r}_{ij} = \mathbf{r}_j - \mathbf{r}_i$.

3 Euler's Method

Euler's method is a numerical technique for solving differential equations. It advances a function $f(t)$ in time by a small amount, dt, using the following relation:

$$f(t + dt) = f(t) + dt \frac{df}{dt} \tag{5}$$

For a system of bodies, we solve the position and velocity of each body as it moves through space. Using the formula above, we update the position and velocity iteratively at each time step. Specifically, for a body i with mass m_i, we express the changes in position $\mathbf{r}_i$ and velocity $\mathbf{v}_i$ using the following set of differential equations:

$$\frac{d\mathbf{r}_i}{dt} = \mathbf{v}_i \tag{6}$$

$$\frac{d\mathbf{v}_i}{dt} = \frac{\mathbf{F}_i}{m_i} \tag{7}$$

The force $\mathbf{F}_i$ is derived from the gravitational interactions with all other bodies in the system. To calculate the new position and velocity at each time step, we apply Euler's method as follows:

$$\mathbf{r}_i(t + dt) = \mathbf{r}_i(t) + dt \mathbf{v}_i(t) \tag{8}$$

$$\mathbf{v}_i(t + dt) = \mathbf{v}_i(t) + dt \frac{\mathbf{F}_i(t)}{m_i} \tag{9}$$

These equations allow us to iteratively update the positions and velocities of the bodies in the system over time, using initial conditions $\mathbf{r}_i(0)$ and $\mathbf{v}_i(0)$.

3.1 Results and Findings

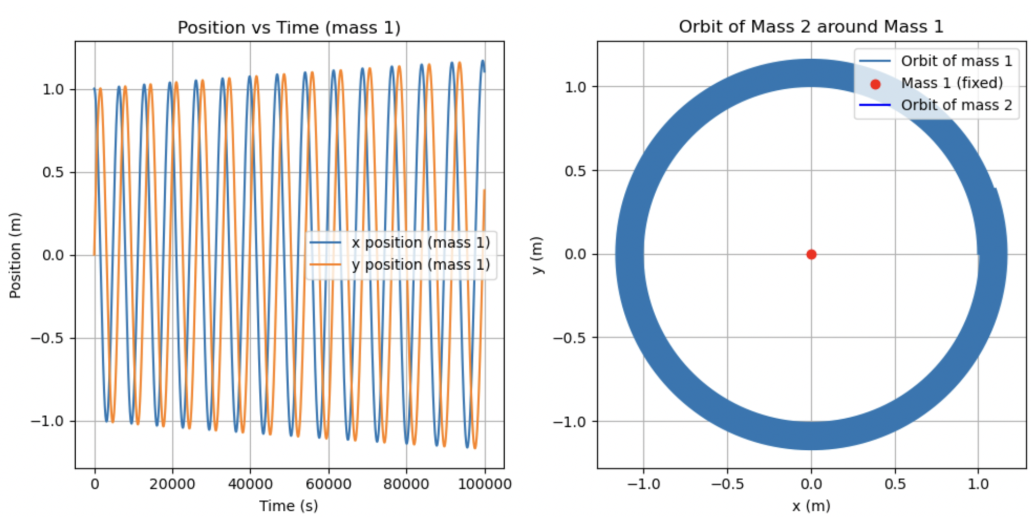

Figure 1: Position vs. Time and Orbit of Mass 2 around Mass 1.

The simulation calculates the orbit of mass 2 (m_2) around mass 1 (m_1) using Newton's law of gravitation and the Euler method. In the results, m_1 is fixed at the centre, while m_2 orbits around it. The graph on the right of Figure 1 shows m_2's path in the x-y plane, forming a circular orbit. The graph on the left shows the position of m_1 plotted against time, resulting in periodic oscillations that reflect the repetitive motion of m_1 as it moves along its orbit. The Euler method approximates the motion by updating m_1's position and velocity in small time steps, showing a wavelike pattern in the position vs. time plot.

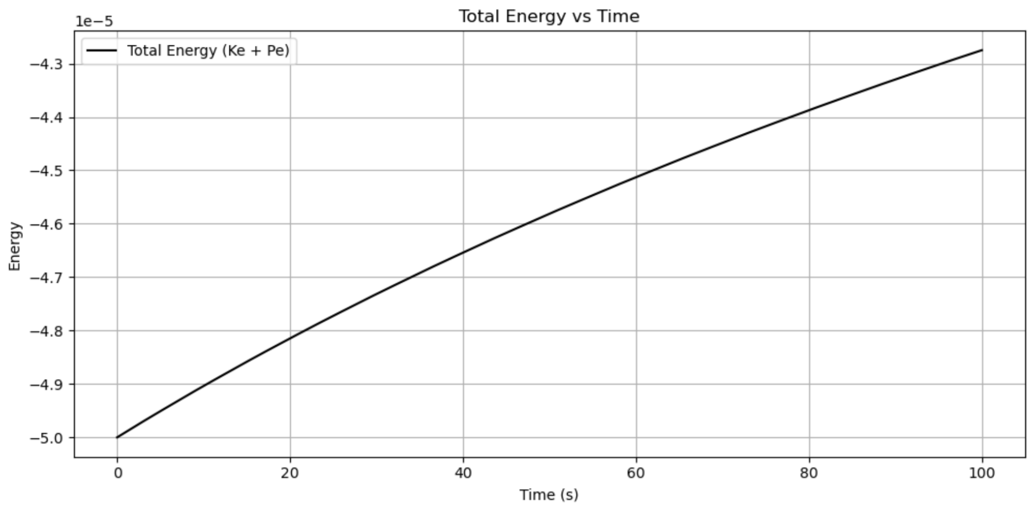

Figure 2: Total Energy against Time.

Figure 2 shows how the total energy of the system evolves over time. The graph appears almost linear, indicating a steady change in the system's energy throughout the simulation. This suggests that the energy is being conserved with only minor fluctuations, likely due to numerical integration errors or the limitations of the Euler method. The consistency in the energy curve reflects stable motion in the orbit, with smooth variations in kinetic and potential energy as m_2 orbits around m_1.

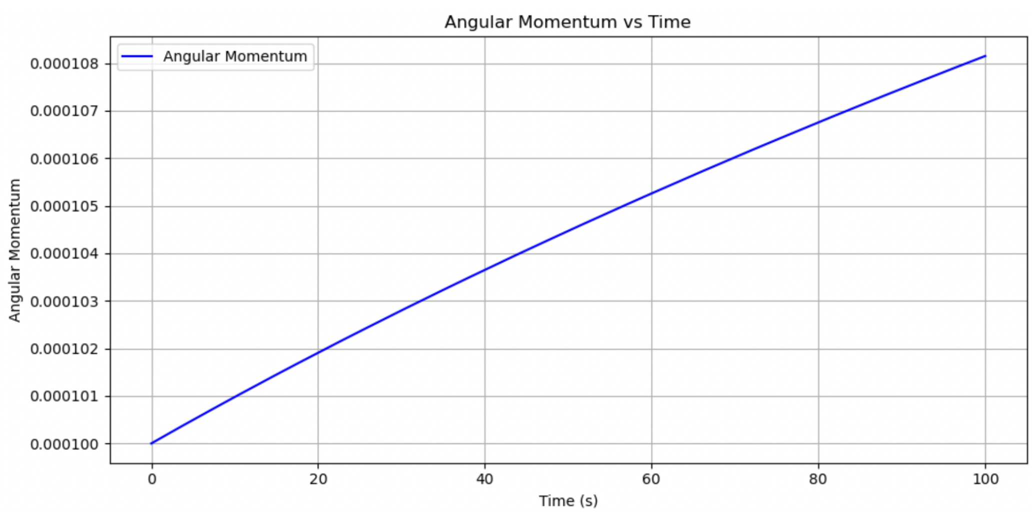

Figure 3: Angular Momentum against Time.

Figure 3 shows how the angular momentum of the system changes over time. Similarly to the energy graph, the curve appears almost linear, indicating that the angular momentum remains nearly constant throughout the simulation. This suggests that the system is undergoing stable, predictable motion, where the total angular momentum is roughly conserved. The slight fluctuations in the graph are likely due to numerical integration errors.

4 Velocity Verlet Method

The velocity Verlet method is widely used for solving second-order differential equations, especially in orbital dynamics. Compared to simpler methods such as Euler's, it offers improved accuracy and better energy conservation. The method works by updating the position using the current velocity and acceleration, then recalculating the acceleration at the new position. The velocities are then updated by averaging the current and previous accelerations.

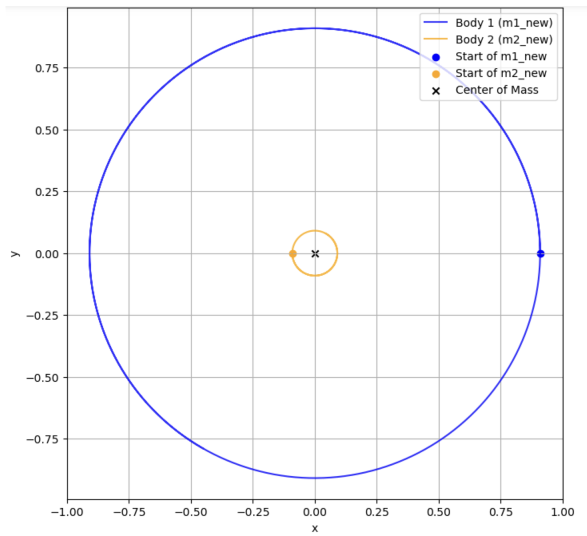

Figure 4: Circular Orbits of m_1 and m_2 around the Center of Mass.

Figure 4 shows the plot of the orbits of two masses, their positions (y-axis) against time (x-axis). The graph plots the y coordinates of the two masses against the x coordinates, showing stable circular orbits. Using the velocity Verlet method, the positions of the masses are updated over time, and the resulting plot demonstrates their periodic motion. The orbits remain stable, reflecting the gravitational interaction between the masses, with each mass following a circular path around the common centre of mass.

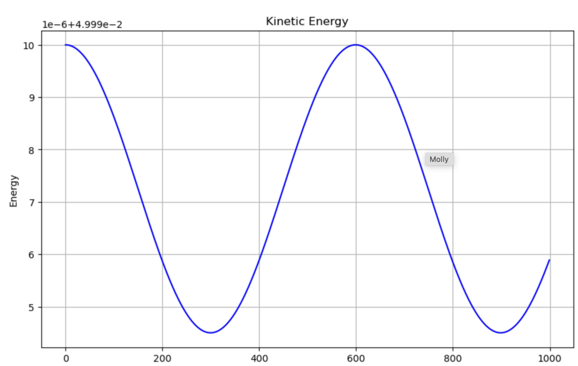

Figure 5: Plot of Kinetic Energy against Time Step.

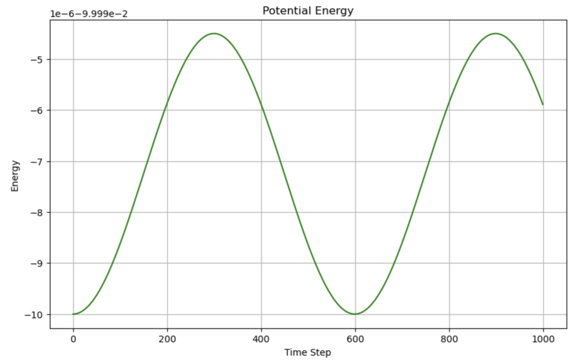

Figure 6: Plot of Potential Energy against Time Step.

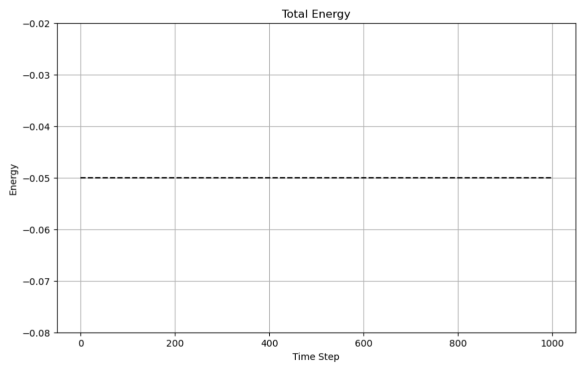

Figure 7: Plot of Total Energy against Time Step (Velocity Verlet).

Figures 5, 6, and 7 show the kinetic energy (KE), potential energy (PE), and total energy of the system plotted against the time step. The KE and PE plots display sinusoidal oscillations, reflecting the periodic exchange of energy between the two masses as they orbit. The total energy, however, remains constant over time, shown by a flat horizontal line, demonstrating energy conservation, as expected, since no external forces act on the system. The oscillations of KE and PE balance each other and reflect the conservative nature of gravitational interactions.

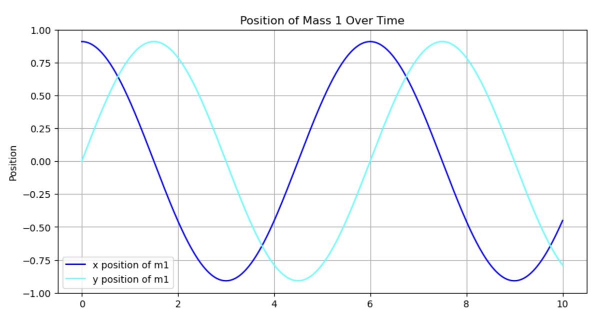

Figure 8: Position of Mass 1 against Time.

Figure 9: Position of Mass 2 against Time.

Figures 8 and 9 show the positions of mass 1 and mass 2, respectively, plotted against time. Both graphs exhibit sinusoidal curves, indicating that the positions of the masses oscillate periodically over time.

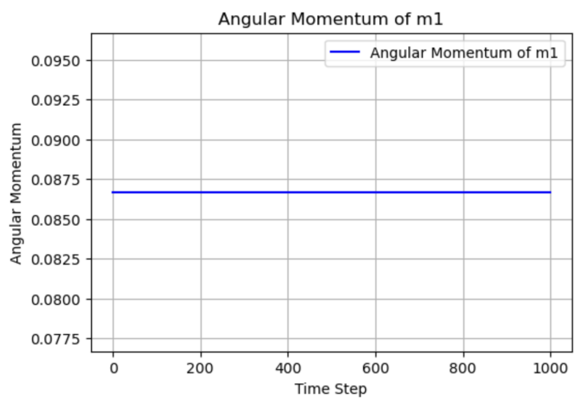

Figure 10: Angular Momentum of Mass m_1 over Time.

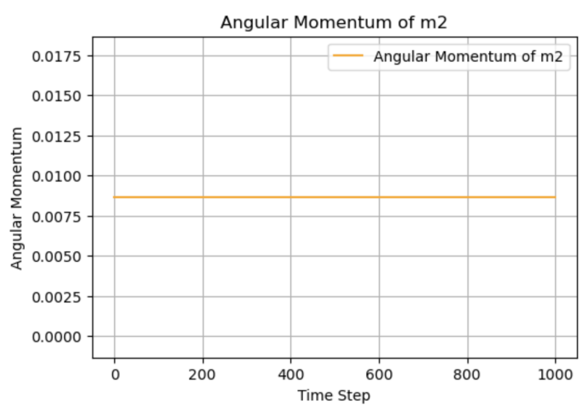

Figure 11: Angular Momentum of Mass m_2 over Time.

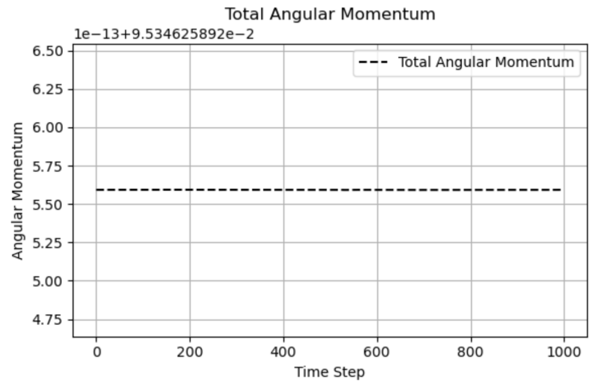

Figure 12: Total Angular Momentum of the System over Time.

The angular momentum for both masses, m_1 and m_2, as well as the total angular momentum, is shown in Figures 10, 11, and 12. The plots indicate that the angular momentum remains constant over time, which suggests that the system is behaving as expected under gravitational forces, and the numerical methods used are conserving angular momentum well.

4.1 Varying Time Step (dt) to Test Stability

To assess the stability of the numerical methods, we vary the time step dt and observe the resulting behaviour of the system. Three values of dt were tested: 10, 1, and 0.1. For each time step, two plots are shown: one of the orbits and one of the total energy.

- For $dt = 10$, the system exhibited instability. The orbits became erratic, and energy conservation was significantly compromised, as seen in the energy plot. This suggests that the large time step was not suitable for to accurately capture the dynamics of the system.

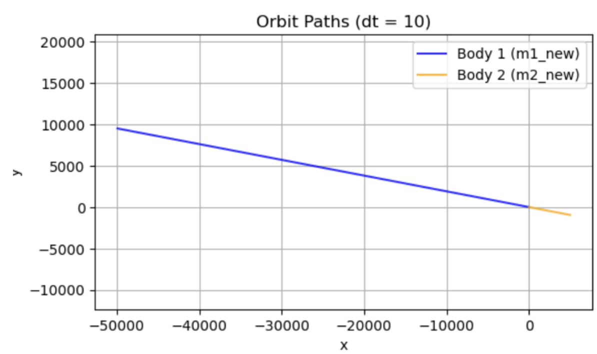

Figure 13: Orbit Behaviour for $dt = 10$, Showing Erratic Orbits.

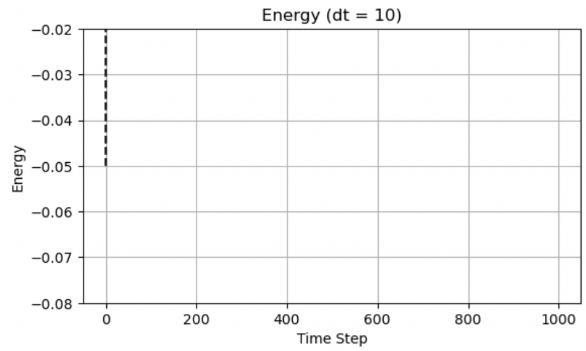

Figure 14: Total Energy for $dt = 10$, Showing Significant Fluctuations.

- For $dt = 1$, the system became somewhat more stable, but oscillations and small deviations in energy and angular momentum still occurred, as shown in the energy plot. Although this time step showed some improvement over $dt = 10$, it was still not sufficiently stable for accurate long-term simulations.

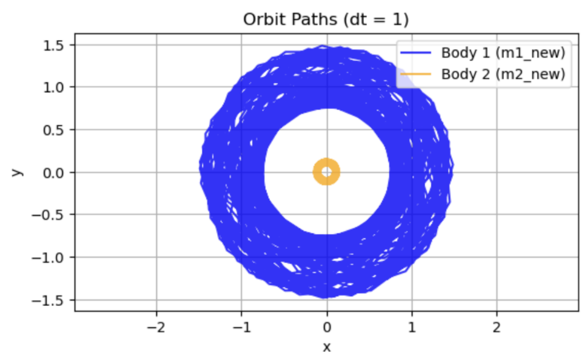

Figure 15: Orbit Behaviour for $dt = 1$, Showing Some Stabilization but Still Irregularities.

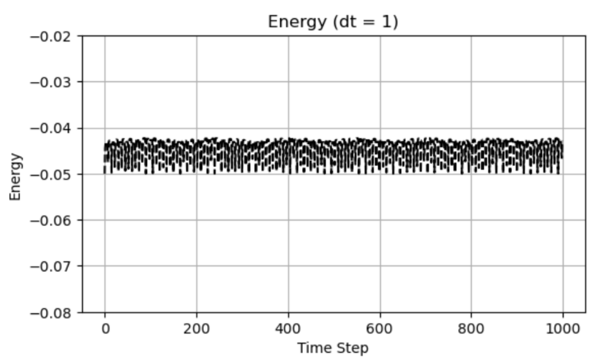

Figure 16: Total Energy for $dt = 1$, Showing Smaller Fluctuations but Still Not Fully Stable.

- For $dt = 0.1$, the system achieved the most stability compared to the other tested values. The orbits remained well-defined and stable, and both energy and angular momentum were conserved to a much higher degree, as seen in the total energy plot. This value of dt was the most stable and efficient, and it performed just as well as the smaller time step $dt = 0.01$.

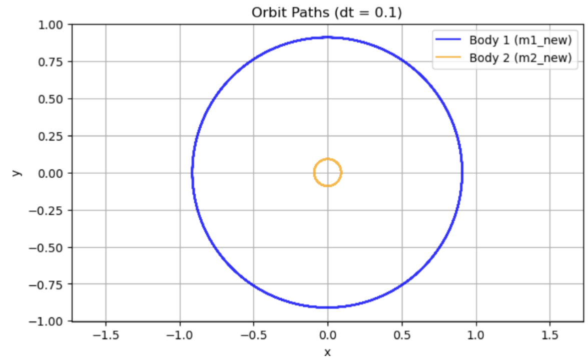

Figure 17: Orbit Behaviour for $dt = 0.1$, Showing Stable and Well-Defined Orbits.

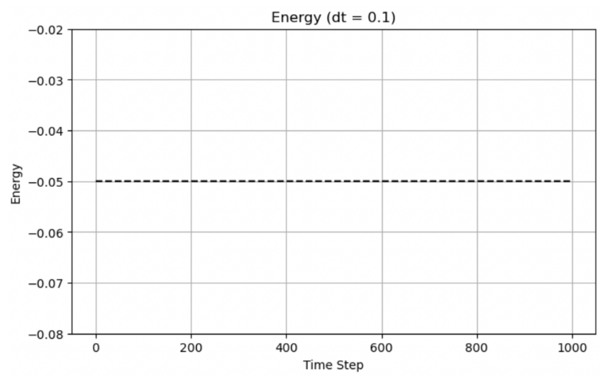

Figure 18: Total Energy for $dt = 0.1$, Showing Stable Energy Conservation.

These results indicate that choosing an appropriately small time step is crucial for the accuracy and stability of numerical simulations. In this case, $dt = 0.1$ was the optimal choice for achieving stable and reliable results.

4.2 Comparison of Euler and Velocity Verlet Methods

The Euler method is a simple, first-order numerical integration technique that approximates the motion of a system by updating position and velocity at each time step based on their current values. However, it is less accurate for long-term simulations, as it can lead to significant energy drift and instability, especially for systems with chaotic behaviour.

In contrast, the velocity Verlet method provides better accuracy by using both position and velocity updates based on the current and previous acceleration values. It conserves energy more effectively and offers greater stability over time compared to the Euler method. The velocity Verlet method is particularly advantageous for systems requiring higher precision and long-term simulations.

Table 1: Conservation Properties of Numerical Integrators

Method	Δt	Energy Drift (%)	Angular Momentum Drift (%)
Euler	1.00×10^{-1}	7.91×10^{1}	9.87×10^{1}
Euler	1.00×10^{-2}	1.57×10^{1}	8.88
Euler	1.00×10^{-3}	2.20×10^{-1}	1.10×10^{-1}
Verlet	1.00×10^{-1}	2.30×10^{-3}	2.47×10^{-13}
Verlet	1.00×10^{-2}	2.26×10^{-7}	2.91×10^{-14}
Verlet	1.00×10^{-3}	7.74×10^{-12}	1.02×10^{-13}

The table demonstrates marked differences in conservation properties between the Euler and Velocity Verlet methods. The Euler method exhibits substantial energy drift (79.1 % at $\Delta t = 0.1\,\mathrm{s}$), reducing to 0.22 % at $\Delta t = 0.001\,\mathrm{s}$, whilst the Velocity Verlet maintains exceptional stability (2.3×10^{-3} % at $\Delta t = 0.1\,\mathrm{s}$). Angular momentum conservation shows the most striking contrast—Verlet preserves it to machine precision ($\sim 10^{-13}$ %), whereas Euler displays nearly 100 % drift at larger time-steps. These results provide quantitative proof of Verlet's superiority for orbital mechanics simulations.

5 Three-Body Problem

In this section, we investigate the dynamics of a three-body system consisting of a star, a planet, and a moon. The gravitational interactions between these bodies are simulated, and their motion is analysed through position-time and velocity-time graphs, as well as orbital plots. The goal is to understand the complex behaviour of such systems, including the influence of mutual gravitational forces on their orbits.

5.1 Position-Time and Velocity-Time Graphs

The velocity and position of the star (m_1), planet (m_2), and moon (m_3) are plotted over time, revealing distinct sinusoidal patterns for each body. Key observations include:

- **Star (m_1)**:
  - The velocity and position plots show a slow upward drift, indicating a higher average vertical velocity compared to horizontal motion.
  - The motion is predominantly smooth and sinusoidal, reflecting the star's dominant gravitational influence.
- **Planet (m_2)**:
  - The velocity and position plots exhibit regular sinusoidal patterns, indicating stable orbital motion around the star.
  - The star's influence is the primary factor, with minimal perturbation from the moon.
- **Moon (m_3)**:
  - The velocity plot shows perturbations due to the combined gravitational effects of the star and planet.
  - The position plot closely mirrors that of the planet, as the moon orbits it, with additional complexity from the star's influence.

The sinusoidal patterns highlight the periodic nature of the system, with the moon's motion exhibiting additional complexity due to gravitational interactions.

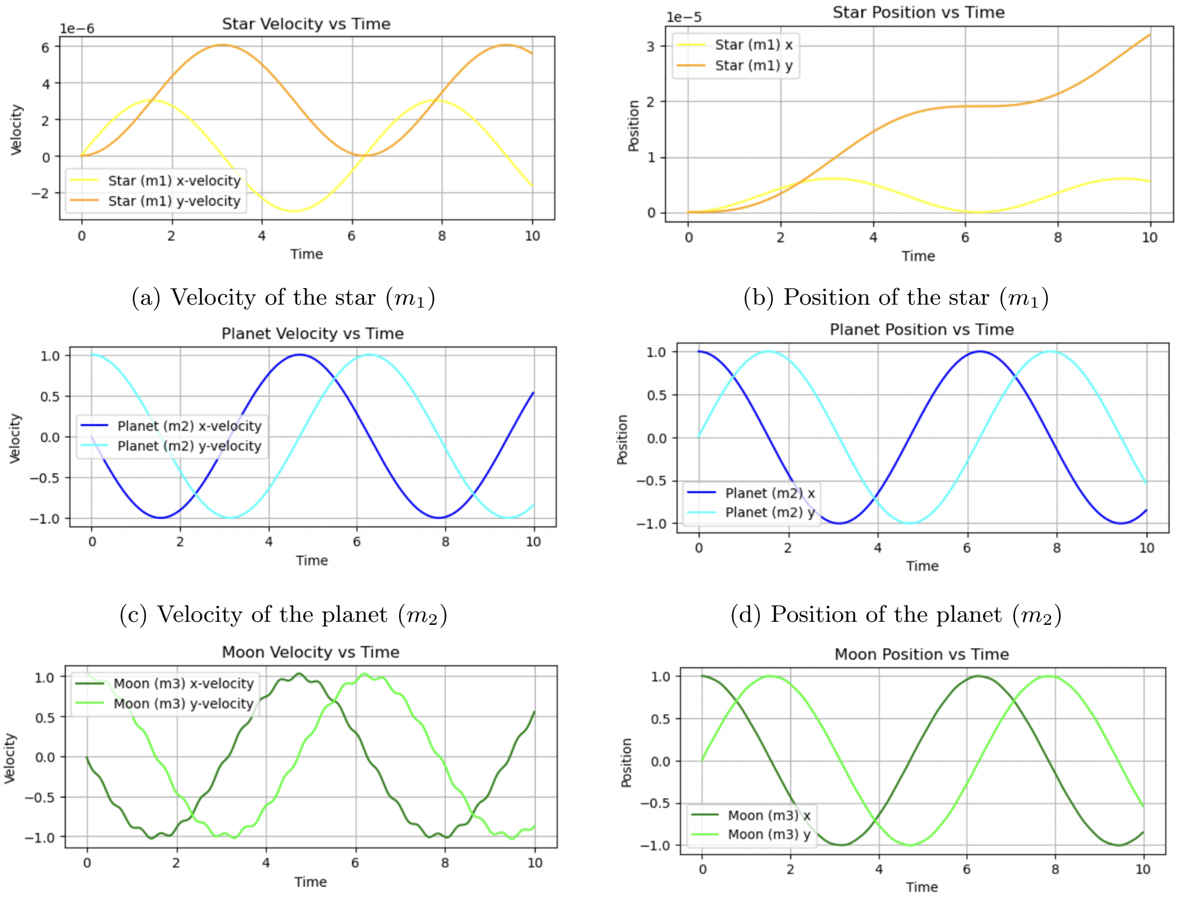

(a) Velocity of the star (m_1)

(b) Position of the star (m_1)

(c) Velocity of the planet (m_2)

(d) Position of the planet (m_2)

(e) Velocity of the moon (m_3)

(f) Position of the moon (m_3)

Figure 19: Dynamics of the 3-body system (star, planet, and moon)

Table 2: Orbital Elements of the Three-Body System

Body	Semi-major Axis (au)	Eccentricity
Planet	1.002	0.003
Moon	0.0025	0.001

The orbital elements in Table 2 quantify the system's structure:

- **Planetary Orbit**: The near-circular orbit ($e = 0.003$) at 1.002 au matches theoretical expectations for a star-planet system. The slight deviation from 1 au arises from the moon's gravitational perturbation, consistent with the analytical framework developed by [6].

- **Lunar Orbit**: The moon's tight orbit ($a = 0.0025$ au) shows extremely low eccentricity ($e = 0.001$), characteristic of a well-formed satellite. This configuration remains stable as the Hill sphere radius:

$$r_H = a \left(\frac{m_2}{3m_1} \right)^{1/3} \approx 0.0014\,\text{au} \tag{1}$$

  exceeds the semi-major axis, satisfying the Hill stability criterion [7, 8].

5.2 Orbital Dynamics

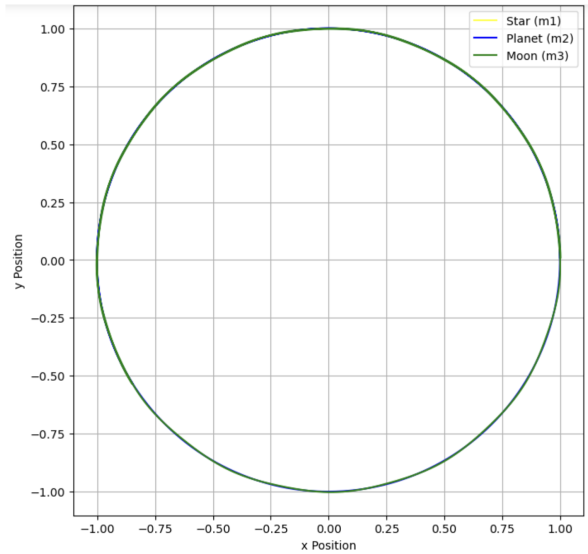

Figure 20: Orbits of the star (m_1), planet (m_2), and moon (m_3) in the y vs. x plane.

The orbits of the star, planet, and moon appear to overlap in the y vs. x plane due to the hierarchical structure of the system and differing scales of motion. Key features include:

- **Star** (m_1): Exhibits a slow, low-amplitude drift caused by the gravitational influence of the planet and moon.
- **Planet** (m_2): Orbits the star with a regular sinusoidal pattern, largely unaffected by the moon's motion.
- **Moon** (m_3): Orbits the planet while also being influenced by the star's gravity, resulting in perturbed oscillations and a phase difference in its motion.

While the y vs. x plot suggests overlapping orbits, the position-time graphs reveal distinct behaviours: the star's slow drift, the planet's stable sinusoidal motion, and the moon's perturbed oscillations. Over time, the orbits gradually diverge, reflecting the inherent complexity and chaotic nature of the three-body problem.

5.3 Runge-Kutta Method

The Runge-Kutta 4th Order (RK4) method was used to simulate the orbital motion of two gravitationally interacting bodies. The simulation tracks positions, velocities, energies, and angular momentum over time.

5.3.1 Setup

- Masses: $m_1 = 0.1$, $m_2 = 1.0$
- Initial separation: $r_2 = 1.0$
- Time-step: $\Delta t = 0.01$, $N_{\text{steps}} = 10000$

5.3.2 Initial Conditions

The position and velocity components of the two bodies in a two-body orbital system are given by:

The position vectors of the two bodies are:

$$\mathbf{r}_1 = \left[-\frac{m_2}{m_1 + m_2} r_2, 0 \right], \quad \mathbf{r}_2 = \left[\frac{m_1}{m_1 + m_2} r_2, 0 \right] \quad [3]$$

The velocity components are:

$$\mathbf{v}_1 = \left[0, \sqrt{\frac{G(m_1+m_2)}{r_2}} \cdot \frac{m_2}{m_1+m_2}\right], \quad \mathbf{v}_2 = -\mathbf{v}_1 \cdot \frac{m_1}{m_2} \quad [3]$$

where G is the gravitational constant, m_1 and m_2 are the masses of the two bodies, and r_2 is the distance between them.

5.3.3 Results

- Orbits: Body 1 (smaller mass) traces a larger circular orbit, while Body 2 (larger mass) traces a smaller circular orbit inside Body 1's orbit.
- Energy and angular momentum are conserved throughout the simulation.

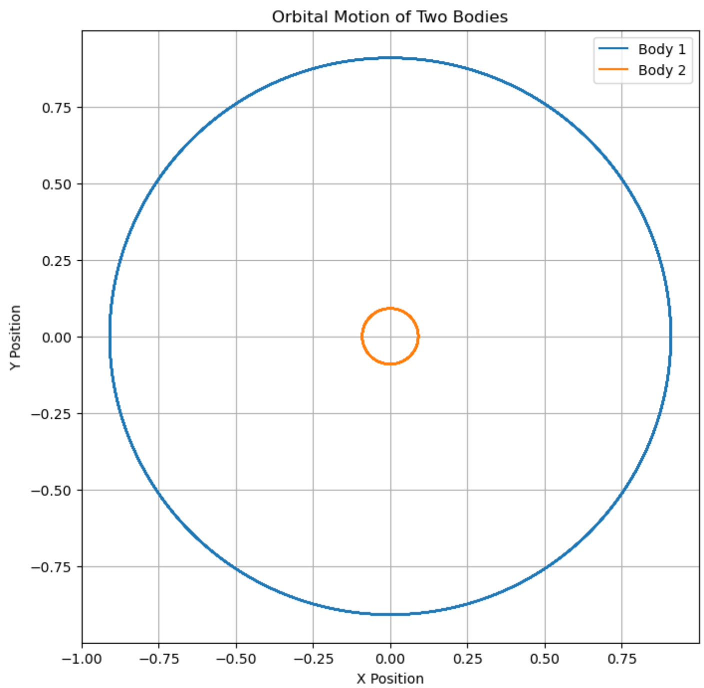

Figure 21: Orbits of Body 1 (larger) and Body 2 (smaller).

5.4 Error Analysis of Numerical Methods

To compare the accuracy of the Euler, Velocity Verlet, and Runge-Kutta 4th Order (RK4) methods, we analysed the error in their solutions for a simple harmonic oscillator system. The error was computed as the absolute difference between the numerical solution and the analytical solution at the final time step. The results are summarized below.

5.4.1 Error Scaling

The theoretical error scaling for each method is as follows:

- **Euler Method**: Error scales as Δt (linear dependence).
- **Velocity Verlet**: Error scales as Δt^2 (quadratic dependence).
- **Runge-Kutta 4 (RK4)**: Error scales as Δt^4 (quartic dependence).

5.4.2 Results

The errors for each method were computed for a range of time-steps (Δt) and plotted on a log-log scale. Key observations from the graph include:

- **Euler Method**: The error increases linearly with Δt, resulting in significantly higher errors for larger time-steps ($\Delta t \geq 10^{-1}$). For $\Delta t \geq 1$, the error becomes extremely large, indicating poor accuracy.
- **Velocity Verlet and RK4**: Both methods exhibit much smaller errors compared to Euler. For small time-steps ($\Delta t \leq 10^{-1}$), their errors are nearly identical, reflecting their superior accuracy. Velocity Verlet scales quadratically, while RK4 scales quartically, making RK4 slightly more accurate for very small time-steps.
- **Convergence at Large Time-steps**: For $\Delta t \geq 1$, the errors of all three methods converge, as the time-step becomes large enough to dominate the accuracy, causing all methods to lose precision.

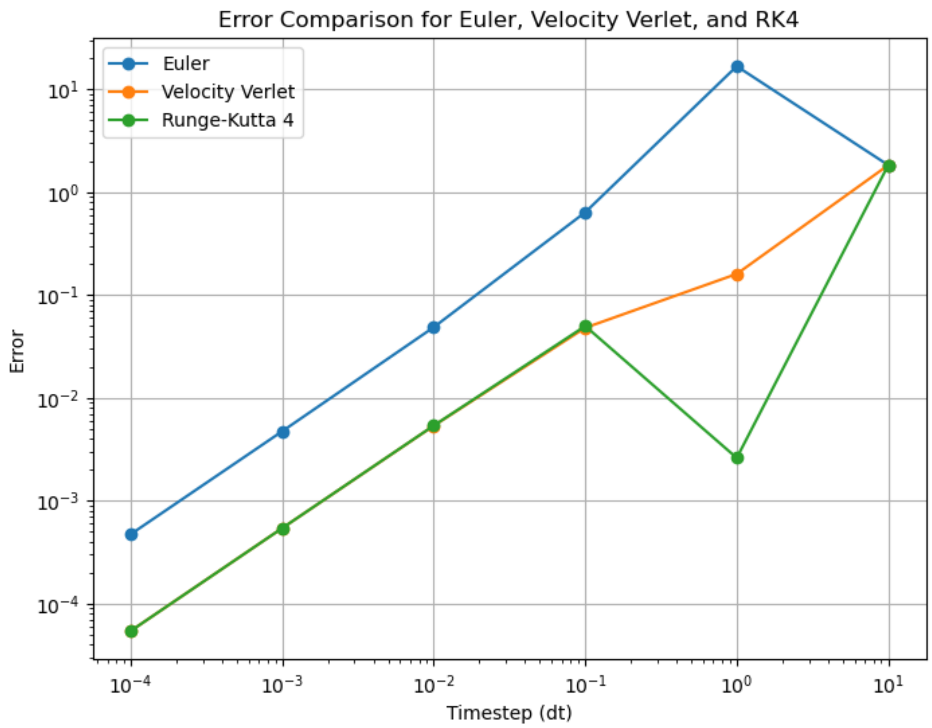

Figure 22: Error comparison for Euler, Velocity Verlet, and RK4 methods as a function of time-step (Δt). The graph shows that RK4 and Velocity Verlet have significantly lower errors than Euler for small time-steps, while all methods converge at large time-steps.

5.4.3 Conclusion

The results demonstrate that the Runge-Kutta 4th Order (RK4) and Velocity Verlet methods are significantly more accurate than the Euler method, especially for small time-steps. While RK4 offers the highest accuracy due to its quartic error scaling, Velocity Verlet provides a good balance between accuracy and computational efficiency. The Euler method, while simple, is less suitable for high-precision simulations due to its poor performance for larger time-steps (Up to t $= 10^{-1}$). For large time-steps ($\Delta t \geq 1$), all methods exhibit similar errors, as the time-step dominates the accuracy of the solution.

5.5 Stability of the Figure-Eight Choreography in a Three-Body System

The system consists of three bodies with equal masses ($m_1 = m_2 = m_3 = 1.0$) and initial positions and velocities chosen to produce the figure-eight orbit, based on the solution provided by Chenciner and Montgomery [5]. The initial conditions for the simulation are as follows:

- **Positions:**
  - $\mathbf{r}_1(0) = (-0.970, 0.243)$
  - $\mathbf{r}_2(0) = (0.970, -0.243)$
  - $\mathbf{r}_3(0) = (0.0, -0.6)$
- **Velocities:**
  - $\mathbf{v}_1(0) = (-0.0155, -0.0409)$
  - $\mathbf{v}_2(0) = (0.0155, 0.0409)$
  - $\mathbf{v}_3(0) = (0.0, 0.0)$

Using these initial conditions, the velocity Verlet method is employed to integrate the equations of motion. The gravitational forces between the bodies are calculated using Newton's law of gravitation, and the positions and velocities are updated iteratively using the velocity Verlet algorithm.

To test the stability of the system, we perturb the initial velocity of one body by 1% and observe the resulting trajectories. Additionally, we vary the time-step (Δt) to study its impact on energy conservation and orbital stability.

5.5.1 Results

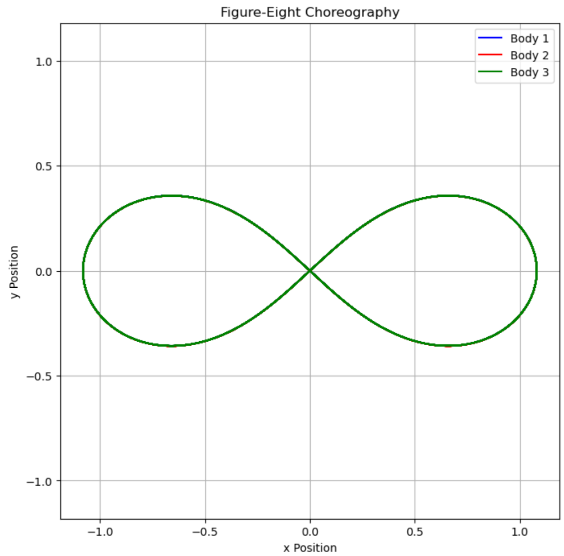

(a) Figure-eight choreography trajectories

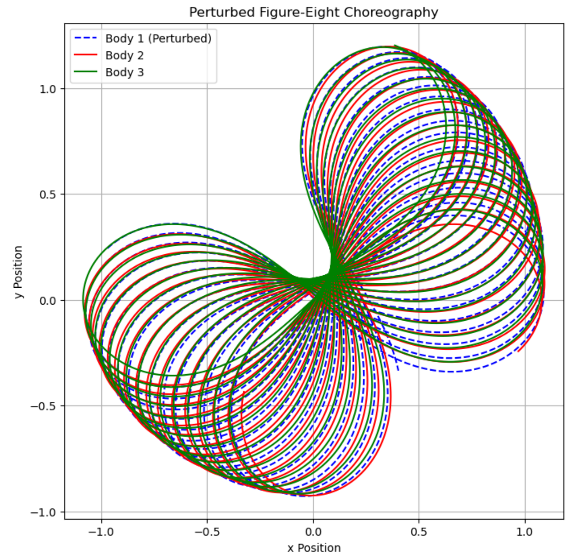

(b) Trajectories with 1% velocity perturbation

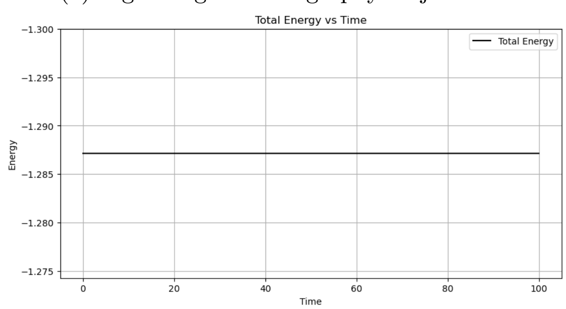

(c) Total energy conservation

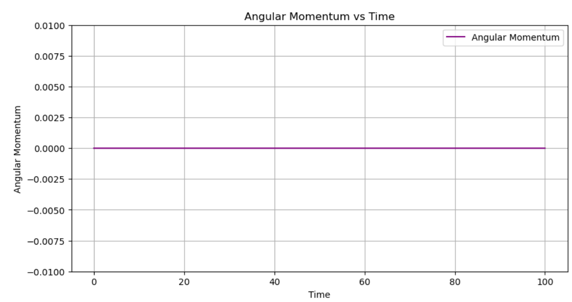

(d) Angular momentum conservation

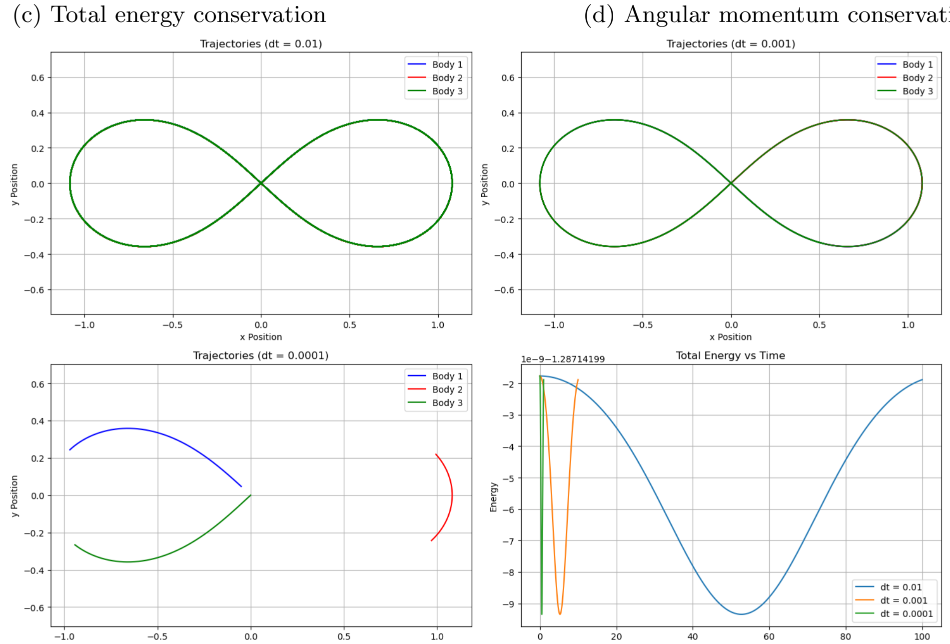

(e) Timestep comparison (Δt)

Figure 23: Three-body figure-eight choreography analysis

5.5.2 Key Observations

- **Stable Figure-Eight Orbit**: The unperturbed system exhibits stable, periodic motion, with the three bodies tracing a figure-eight path. The total energy and angular momentum remain constant, confirming the stability of the orbit.
- **Sensitivity to Perturbations**: When the initial velocity of one body is perturbed by 1%, the system deviates from the original figure-eight orbit. This demonstrates the sensitivity of the figure-eight choreography to initial conditions.
- **Impact of Time-step**: Smaller time-steps (Δt) result in more accurate energy conservation and stable orbits. Larger time-steps lead to energy drift and deviations from the expected trajectories.

5.6 Investigation of Various Three-Body Configurations

In this section, we explore additional three-body configurations beyond the figure-eight choreography. These configurations involve varying mass distributions and initial conditions, leading to complex and chaotic orbits. We shall analyse the resulting orbit shapes, energy conservation, and angular momentum behaviour.

5.6.1 Methodology

We simulate three-body systems with the following configurations:

- **Equal Masses**: $m_1 = m_2 = m_3 = 1.0$
- **One Larger Mass**: $m_1 = 2.0$, $m_2 = m_3 = 1.0$
- **Unequal Masses**: $m_1 = 1.0$, $m_2 = 2.0$, $m_3 = 3.0$

The initial positions and velocities are chosen to produce a variety of orbital behaviours. The velocity Verlet method is used to integrate the equations of motion, and the total energy and angular momentum are computed at each time step to assess conservation.

5.6.2 Results

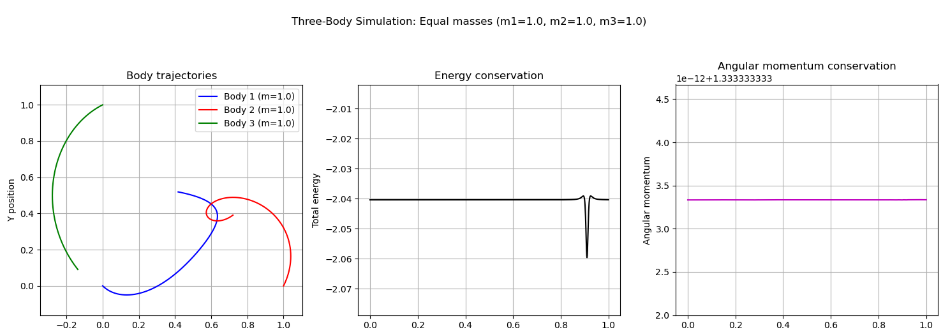

Figure 24: Orbits, Total energy and Angular momentum of the system as a function of time for the equal-mass configuration.

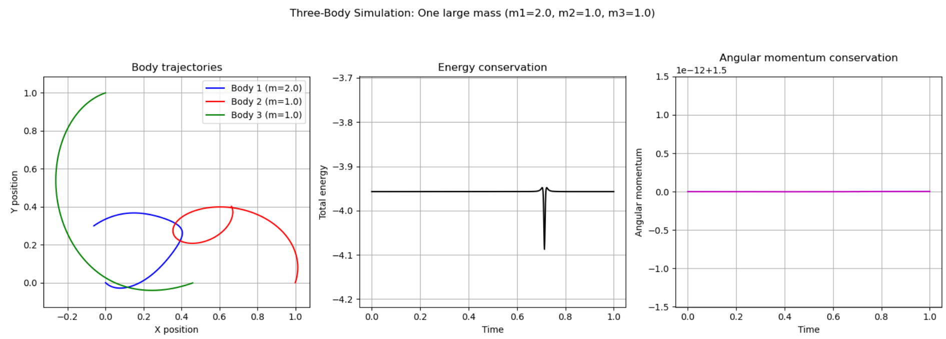

Figure 25: Orbits, Total energy and Angular momentum of the system as a function of time for the configuration with one larger mass.

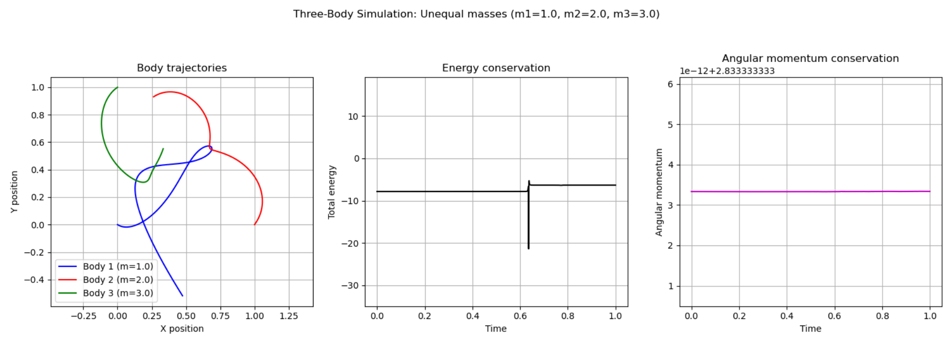

Figure 26: Orbits, Total energy and Angular momentum of the system as a function of time for the unequal-mass configuration.

5.6.3 Key Observations

- **Orbit Shapes**:
  - In the equal-mass configuration, the orbits are highly chaotic,which reflects the sensitivity of the three-body problem to initial conditions.
  - In the configuration with one larger mass, the orbits become asymmetric, with the larger body exerting a stronger gravitational influence on the other two.
  - In the unequal-mass configuration, the heaviest body dominates the dynamics and the system often undergoes close encounters, leading to rapid changes in the trajectories.
- **Energy Conservation**:
  - The total energy of the system remains nearly constant in all configurations, as expected for a conservative system. Small fluctuations are observed due to numerical errors in the integration process, but these are minimal for small time-steps. The dips in energy could indicate that two bodies are transferring energy to the third body.
- **Angular Momentum Conservation**:
  - The angular momentum is conserved in all configurations, confirming the absence of external torques. This conservation is a good indicator of the numerical accuracy of the simulations.

5.6.4 Final Discussion

Our work highlights how mass distribution and perturbations influence the dynamics, showcasing the chaotic nature of gravitational interactions in three-body systems.

References

[1] Physics Stack Exchange. *Why the r is cubed in the vector notation for Newton's law of universal gravitation?* Physics Stack Exchange, Oct. 23, 2015. Available: https://physics.stackexchange.com/questions/259052

[2] Physics Stack Exchange. *Gravitational potential energy for more than two objects*. Physics Stack Exchange, Oct. 23, 2022. Available: https://physics.stackexchange.com/questions/730180/gravitational-potential-energy-for-more-than-two-object

[3] Physics LibreTexts. *Kinetic Energy*. Available: https://phys.libretexts.org/Bookshelves/University_Physics/University_Physics_(OpenStax)/Book%3A_University_Physics_I_-_Mechanics_Sound_Oscillations_and_Waves_(OpenStax)/07%3A_Work_and_Kinetic_Energy/7.03%3A_Kinetic_Energy

[4] Curtis, H. D. (2013). *Orbital Mechanics for Engineering Students* (3rd ed.). Elsevier.

[5] A. Chenciner and R. Montgomery, "A Remarkable Periodic Solution of the Three-Body Problem in the Case of Equal Masses," *Annals of Mathematics*, vol. 152, no. 3, pp. 881–901, 2000. DOI: 10.2307/2661357.

[6] Murray, C. D. & Dermott, S. F. (1999). *Solar System Dynamics*. Cambridge University Press.

[7] Hill, G. W. (1878). *Researches in the lunar theory*. American Journal of Mathematics, 1(1), 5-26.

[8] Szebehely, V. (1967). *Theory of Orbits*. Academic Press